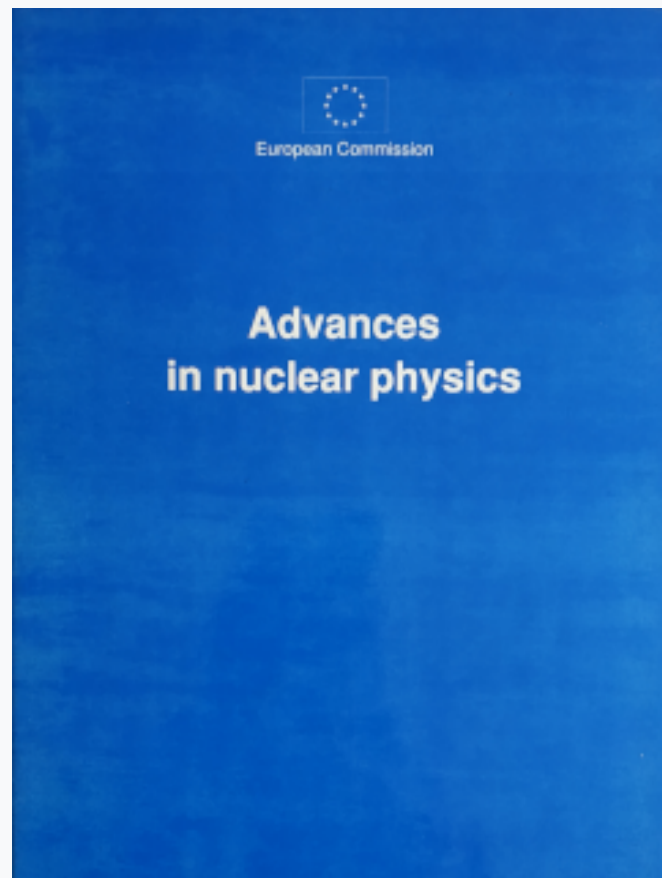


HNPS Advances in Nuclear Physics

Vol 5 (1994)

HNPS1994



**Inclusive neutrino-nucleus reaction cross sections
at intermediate energies**

T. S. Kosmas, E. Oset

doi: [10.12681/hnps.2892](https://doi.org/10.12681/hnps.2892)

To cite this article:

Kosmas, T. S., & Oset, E. (2020). Inclusive neutrino-nucleus reaction cross sections at intermediate energies. *HNPS Advances in Nuclear Physics*, 5, 29–41. <https://doi.org/10.12681/hnps.2892>

Inclusive neutrino-nucleus reaction cross sections at intermediate energies¹

T. S. KOSMAS¹ and E. OSET²

*¹ Division of Theoretical Physics, University of Ioannina, GR-451 10 Ioannina,
Greece*

*² Departamento de Fisica Teorica, Universidad de Valencia, 46100, Burjassot,
Valencia, Spain*

Abstract

Inclusive neutrino-nucleus reaction cross sections at intermediate energies ($20\text{MeV} \leq E_\nu \leq 500\text{MeV}$) are calculated throughout the periodic table for the most interesting nuclei from an experimental point of view. The method used had previously proved to be very accurate in calculating the induced reaction cross section for $T=0$ light nuclei (^{12}C and ^{16}O) and in the study of other similar processes like the ordinary muon capture. The electron-neutrino (ν_e) cross section weighted by the Michel distribution is also discussed in conjunction with the existing experimental results at LAMPF and KARMEN.

I. INTRODUCTION

The study of neutrino-nucleus cross sections is of great importance in neutrino detection [1]-[6] in particular for nuclear targets used in the existing neutrino detectors [7]-[11] and promising nuclear isotopes recently proposed to be used as neutrino detection targets [9],[12]-[20]. In the low neutrino-energy regime ($E_\nu \leq 20\text{MeV}$), which includes the solar neutrinos and the low-energy supernova neutrinos [21], detectors need low threshold energy targets; such targets used in detectors being in operation are the ^{37}Cl in Davis experiment at Homestake [1,6] and the ^{71}Ga in Gallex experiment at Gran Sasso [8] and in SAGE experiment at Baksan [10]. At intermediate ($20\text{MeV} \leq E_\nu \leq 50\text{MeV}$) and high-neutrino energies ($E_\nu \geq 50\text{MeV}$), the detected neutrinos are produced either during a solar flare [22] or in secondary cosmic rays (atmospheric neutrinos); for observing these more energetic neutrinos, nuclear targets with bigger threshold energy can be used. We mention that the neutrinos of a solar-flare give rise to neutrino energies of some hundred MeV or even in the GeV regime and the neutrinos coming from stellar collapses are considered to have energies $E_\nu \approx 100\text{MeV}$. Neutrinos of such energy may excite a great number of nuclear states as e.g. in the IMB and Kamiokande water detectors [23,24].

¹Presented by T. S. Kosmas.

For the existing detectors it is interesting to know reliable estimates of the neutrino-nucleus reaction cross section for E_ν at least up to a few hundred MeV, e.g. for the radiochemical experiments we need semi-inclusive cross-sections for ^{37}Cl , while for the Cerenkov or liquid scintillation experiments we need inclusive reaction cross sections for ^{16}O , ^{12}C or ^{13}C . On the other hand, for reactions of neutrinos with some nuclei proposed as promising nuclear targets in neutrino detectors like ^{81}Br [14,15], ^{98}Mo [16,17], ^{115}In [12,16], ^{127}I [18,19,20], ^{205}Tl [17], the knowledge of a reliable cross section calculation is a fundamental prerequisite.

So far, inclusive or semi-inclusive neutrino-nucleus cross sections have been calculated for some nuclear targets (^{12}C , ^{16}O , etc.) by using the following methods:

(i) Term-by-term sum [25,26,27]: This method needs the explicit construction of the final nuclear states in the context of a nuclear model and it is reliably applicable for low neutrino energies for light and medium nuclei. In this case transition to definite nuclear states, i.e. to the ground state or to some low-lying nuclear excitations, could be dominant and one has to calculate the exact final state in order to find the partial transition rate.

(ii) Closure approximation [28,29]: With this method one avoids the tedious calculation of the excited nuclear states if the momentum of the outgoing lepton can be approximately determined by means of a suitable mean nuclear excitation energy \bar{E} . Since the results of the closure depend on the assumed value of \bar{E} , the method is more reliable for neutrino-energies $50\text{MeV} \leq E_\nu \leq 100\text{MeV}$.

(iii) Fermi gas models [30,31]: The use of the non-relativistic as well as the relativistic Fermi gas model needs a choice of the average binding energy which defines the effective energy transfer to the nuclear target. The results are very sensitive to the average binding energy used (in particular at low neutrino energies) and more reliable estimates for total neutrino cross sections can be obtained for $E_\nu \geq 50\text{MeV}$ where the details of the specific nuclear states can be ignored.

(iv) Recently [4,32], a new method has been developed in which the differential neutrino-nucleus cross section can be expressed as a function of the local Fermi momentum $p_F(r)$, i.e., by using a local density approximation. In this way both bound as well as excited states of the proton and neutron can be taken into consideration by using the particle-hole excitations included in a relativistic Lindhard function [32,33]. In addition, one can also consider the effects of Coulomb distortion and renormalization of the operators involved in the elementary neutrino-nucleon process inside the nucleus. The latter have been proved to be very important [33,34]. Since the method uses for the total cross section an integration over a continuum of excited states, the results obtained are accurate for neutrino energies $E_\nu \geq 50\text{MeV}$ in the region of light nuclei and for $E_\nu \geq 20\text{MeV}$ in the region of medium and heavy nuclei.

In the present work we have calculated total cross sections for the inclusive neutrino and antineutrino reactions

$$\nu_l + (A, Z) \rightarrow l^- + X, \quad \bar{\nu}_l + (A, Z) \rightarrow l^+ + X, \quad l = e, \mu \quad (1)$$

by using the method (iv) [4]. We have done a systematic study of the total neutrino-nucleus cross sections for the most important nuclear isotopes from an experimental point of view in the neutrino energy region $20\text{MeV} \leq E_\nu \leq 500\text{MeV}$. These neutrino-

energies, which cover the high energy supernova neutrinos ($20\text{MeV} \leq E_\nu \leq 50\text{MeV}$), the solar flare neutrinos ($50\text{MeV} \leq E_\nu \leq 500\text{MeV}$) etc., can excite good enough nuclear states such that, the integration over the continuum involved in the method used here is a very good approximation.

The inclusive neutrino cross sections calculated in the present work, are very important in the study of atmospheric neutrinos which carry neutrino-energies between a few MeV to some GeV and can be observed, e.g. in a large water Cerenkov detector. Such neutrinos are produced from successive reactions which take place when cosmic rays strike the atmosphere by means of the decay of pions, kaons and muons. We also recall that the interesting quantity of the ratio of the muonic-neutrino flux to that of the electronic-neutrino flux for atmospheric neutrinos measured in a Cerenkov counter can be calculated by using the results of the total neutrino cross sections.

From the neutrino cross sections obtained, we can calculate the experimentally important "flux averaged cross section" and compare it with the corresponding values found for various electron-neutrino reactions in KARMEN [36,37] and LAMPF [38] laboratories.

In this work at first we briefly present the relevant formalism and discuss the main steps followed by the method (iv) in order to calculate the inclusive cross sections for a nuclear target. Then we describe the characteristics of the most important neutrino- and antineutrino- nucleus reactions studied here and finally we present and discuss the results obtained for a set of nuclear isotopes including the already employed targets in neutrino detection experiments.

II. BRIEF DESCRIPTION OF THE FORMALISM

For the neutrino-induced reactions of eq. (1) the effective transition operator H_{eff} can be written in a covariant form as

$$H_{eff} = \frac{G \cos \theta_c}{\sqrt{2}} j^\mu J_\mu \quad (2)$$

where G is the weak coupling constant ($G = 1.1664 \times 10^{-5}\text{GeV}^{-2}$) and θ_c the Cabibbo angle ($\cos \theta_c = .974$). The leptonic current j^μ is the familiar one

$$j^\mu = \bar{u}_l(p_l) \gamma^\mu (1 - \gamma_5) u_\nu(p_\nu) \quad (3)$$

where u_ν , u_l are Dirac spinors normalized to m_l/E_l for the neutrino and lepton with four momentum p_ν , p_l , respectively. The hadronic current J_μ in eq. (2) is given by [4]

$$J_\mu = \bar{u}_p(p_p) \left[F_1(q^2) \gamma_\mu + F_2(q^2) i \sigma_{\mu\lambda} \frac{q^\lambda}{2M} + F_A(q^2) \gamma_\mu \gamma_5 + F_P(q^2) q_\mu \gamma_5 \right] u_n(p_n) \quad (4)$$

(M is the nucleon mass). The functions of the four momentum transfer q^2 (with $q = p_p - p_n$): F_1 , F_2 , F_A and F_P are the well known Dirac, Pauli, axial vector and pseudoscalar form factors, respectively. In the convention used in the present work q^2 is written as

$$q^2 = q^\mu q_\mu = q_0^2 - \mathbf{q}^2 = (E_l - E_\nu)^2 - (\mathbf{p}_l - \mathbf{p}_\nu)^2 \quad (5)$$

\mathbf{p}_i denotes the three-momentum of the particles involved in the process.

For the anti-neutrino induced reaction the leptonic and hadronic currents are the complex conjugates of eqs. (3) and (4), respectively.

A. The local density approximation

The calculation of the total neutrino-nucleus reaction cross section σ , according to the method (iv) mentioned in the introduction, is based on the equation [4]

$$\sigma = -\frac{2G^2 \cos^2 \theta_c}{\pi} \int_0^R r^2 dr \int_{p_l^{\min}}^{p_l^{\max}} p_l^2 dp_l \int_{-1}^1 d(\cos \theta) \frac{1}{E_\nu E_l} \bar{\sum} \sum |T|^2 \times \text{Im} \bar{U}(E_\nu - E_l - Q - V_C(r), \mathbf{q}) \Theta(E_l + V_C(r) - m_l) \quad (6)$$

where the quantity $\bar{\sum} \sum |T|^2$ represents the sum over final spins of the leptons averaged over the initial ones (for the analytic form of $|T|^2$ see appendix of ref. [4]). The function $\Theta(E_l + V_C(r) - m_l)$ is the well known *theta* function, V_C is the Coulomb energy of the lepton and Q is the Q -value of the process. The function $\text{Im} \bar{U}(q^0, \mathbf{q})$ represents the imaginary part of the Lindhard function which contains the particle-hole excitations of proton-neutron type. The minimum ($p_l^{\min} = 0$) and maximum ($p_l^{\max} = ((E_l^{\max})^2 - m_\mu^2)^{1/2}$) lepton momentum are determined by the kinematics i.e.

$$E_l^{\max} = E_\nu + \left[\frac{p_{F_n}^2}{2M_n} - \frac{p_{F_p}^2}{2M_p} - V_C(r) - Q \right] \quad (7)$$

In the local density approximation, the magnitude of the momenta p_{F_n} and p_{F_p} are given in terms of the neutron and proton nuclear densities, $\rho_n(r)$ and $\rho_p(r)$, respectively, as

$$p_{F_n} = [3\pi^2 \rho_n(r)]^{1/3}, \quad p_{F_p} = [3\pi^2 \rho_p(r)]^{1/3} \quad (8)$$

In a good approximation ρ_n and ρ_p are obtained from the total charge density of the nucleus $\rho(r)$ via the relations: $\rho_n(r) = \frac{N}{A} \rho(r)$ and $\rho_p(r) = \frac{Z}{A} \rho(r)$. In eq. (6) R takes the value $R = C_1 + 5 \text{ fm}$ where C_1 represent the radius parameter of a two parameter Fermi density distribution (see table 1 below).

In the case of the neutrino reaction of eq. (1) the total energies of the neutron (E_n) and proton (E_p) are written as

$$E_n = \sqrt{\mathbf{p}_n^2 + M_n^2}, \quad E_p = \sqrt{(\mathbf{p}_n + \mathbf{q})^2 + M_p^2} \approx \sqrt{\mathbf{p}_n^2 + \mathbf{q}^2 + M_p^2} \quad (9)$$

where the approximation in E_p holds if $\mathbf{q} \cdot \mathbf{p}_n \approx 0$ (forward scattering conditions).

For the antineutrino-nucleus process, since in this case the role of the proton and neutron is interchanged (we neglect the proton-neutron mass difference), one can calculate the cross section by using the same expression for $|T|^2$ as for neutrino scattering and changing the sign of terms involving the products $F_1 F_A$ and $F_2 F_A$ in the expression of the appendix of ref. [4].

The renormalization of the currents mentioned in the introduction is done by allowing the propagation of the ph in the nuclear medium. The ph response is substituted by an RPA response accounting for ph and delta-hole components which interact by means of

the spin isospin effective nuclear interaction [4]. This renormalization procedure took good account of the renormalization of the currents in muon capture [33] and in beta decay [39].

B. Michel Distribution

The neutrino beams used in experiments (e.g. at LAMPF, KARMEN etc.) are produced from the decay of muons resulting from the decay of slow pions and therefore they have relatively low energies. Such neutrinos do not constitute a monochromatic beam. Their energy distribution is approximately described by the Michel distribution

$$\frac{dN_\nu}{dE_\nu} \equiv W(E_\nu) \approx E_\nu^2 (E_\nu^{\max} - E_\nu) \quad (10)$$

where

$$E_\nu^{\max} \approx \frac{m_\mu^2 - m_e^2}{2m_\mu} \quad (11)$$

For comparison of the theoretical seminclusive cross section with experimental data we can calculate the static quantity of the flux averaged cross section given by

$$\bar{\sigma} = \frac{\int_0^{E_\nu^{\max}} \sigma(E_\nu) W(E_\nu) dE_\nu}{\int_0^{E_\nu^{\max}} W(E_\nu) dE_\nu} \quad (12)$$

The numerator of eq. (12) represents the folding of the neutrino cross section with the energy distribution of eq. (10). The denominator stands for normalization requirements. The maximum energy in the upper limit of this integral is $E_\nu^{\max} \approx 52.8 \text{ MeV}$ (see eq. (10)).

III. NEUTRINO DETECTION REACTIONS

In the present work we have calculated the neutrino cross sections for a series of low-energy β -emitters which are important in neutrino detection. We summarize here the main characteristics of each target nucleus.

^{37}Cl : The ^{37}Cl detector at Homestake being in operation since many years ago [7,9] is based upon the process $^{37}\text{Cl}(\nu_e, e^-)^{37}\text{Ar}$ and is sensitive only to neutrino energies above $E_\nu = .814 \text{ MeV}$. The cross sections measured from the ^{37}Cl neutrino detector can be related with the measured counting rates in the $^{37}\text{Cl}(p, n)^{37}\text{Ar}$ [9,40] reaction in order to obtain the G-T strengths to states in ^{37}Ar .

^{40}Ar : The isotope ^{40}Ar is referred [5] as a useful neutrino detection target for separate neutral current and charged current measurements.

^{71}Ga : The ^{71}Ga was proposed [2] as low threshold target for neutrino detection. Now two $\text{Ga} - \text{Ge}$ detectors at Baksan [13] and Gran Sasso [8] are in operation. Solar neutrino capture via the reaction $^{71}\text{Ga}(\nu_e, e^-)^{71}\text{Ge}$ has a threshold of only $.233 \text{ MeV}$ and has been used as an alternative reaction to determine whether the discrepancy of Davis experiment is due to our misunderstanding of the solar interior or to our incomplete knowledge of the neutrino propagation. In ref. [13] the contributions of the excited states

to the total solar-neutrino capture rate for ^{71}Ga have been studied and the measured capture rates of the p-n reaction $^{71}Ga(p, n)^{71}Ge$ at proton bombarding energies 120 MeV and 200 MeV have been used to extract the total G-T strength function in ^{71}Ge . Also Bahcall [2] estimated small contributions to the total capture cross sections from low lying excited states in ^{71}Ge on the basis of β -decay calculations $^{71}Ga(\beta^+)^{71}Ge$.

^{81}Br : For the important role played by the ^{81}Br detector in solar neutrino spectroscopy see ref. [14,15]. Here we only stress that ^{81}Br is most sensitive to 8B neutrinos and that from solar neutrino capture on ^{81}Br one can deduce the G-T transition strengths for the accessible final states of ^{81}Kr . The threshold energy of the ^{81}Br detector is $E_{thres} = .471 MeV$.

^{98}Mo : The promising ^{98}Mo detector [16,17] offers a unique opportunity to measure the flux of 8B neutrinos. In ref. [16] the 8B neutrino absorption cross section in ^{98}Mo leading to particle stable final states of ^{98}Tc were found to be about 3.5 times larger than that suggested by Cowan and Haxton [17]. The threshold for the neutrino reaction $^{98}Mo(\nu_e, e^-)^{98}Tc$ is $E_{thres} = 1.68 MeV$ but effectively $E_{thres} > 1.74 MeV$ because the ground state and the first excited state of ^{98}Tc are strongly hindered.

Table 1. *Characteristics of some neutrino- and antineutrino-nucleus reactions employed in neutrino detection. The parameters C_1 and C_2 describe a two-parameter Fermi density distribution of the target nucleus and Q (in MeV) represents the Q -value of the corresponding reaction.*

Nucleus	Density Parameters		Neutrino processes		Antineutrino processes	
	$^A_N X$	C_1	C_2	Reaction	Q	Reaction
$^{37}_{17}Cl$	3.535	0.524	$^{37}_{17}Cl(\nu_l, l^-)^{37}_{18}Ar$.303	$^{37}_{17}Cl(\bar{\nu}_l, l^+)^{37}_{16}S$	5.365
$^{40}_{18}Ar$	3.530	0.542	$^{40}_{18}Ar(\nu_l, l^-)^{40}_{19}K$.994	$^{40}_{18}Ar(\bar{\nu}_l, l^+)^{40}_{17}Cl$	8.006
$^{71}_{31}Ga$	4.445	0.580	$^{71}_{31}Ga(\nu_l, l^-)^{71}_{32}Ge$	-.276	$^{71}_{31}Ga(\bar{\nu}_l, l^+)^{71}_{30}Zn$	3.328
$^{81}_{35}Br$	4.640	0.572	$^{81}_{35}Br(\nu_l, l^-)^{81}_{36}Kr$	-.189	$^{81}_{35}Br(\bar{\nu}_l, l^+)^{81}_{34}Se$	2.096
$^{98}_{42}Mo$	5.107	0.569	$^{98}_{42}Mo(\nu_l, l^-)^{98}_{43}Tc$	1.169	$^{98}_{42}Mo(\bar{\nu}_l, l^+)^{98}_{41}Nb$	4.074
$^{115}_{49}In$	5.357	0.563	$^{115}_{49}In(\nu_l, l^-)^{115}_{50}Sn$	-1.005	$^{115}_{49}In(\bar{\nu}_l, l^+)^{115}_{48}Cb$	1.959
$^{127}_{53}I$	5.405	0.552	$^{127}_{53}I(\nu_l, l^-)^{127}_{54}Xe$.152	$^{127}_{53}I(\bar{\nu}_l, l^+)^{127}_{52}Te$	1.206
$^{205}_{81}Tl$	6.495	0.540	$^{205}_{81}Tl(\nu_l, l^-)^{205}_{82}Pb$	-.451	$^{205}_{81}Tl(\bar{\nu}_l, l^+)^{205}_{80}Hg$	2.049

^{115}In : The ^{115}In isotope has been proposed [12] as a target to detect solar neutrinos by means of the reaction $^{115}In(\nu_e, e^-)^{115}Sn$ because it has a very low threshold $E_{thres} = .119\text{MeV}$. The produced ^{115}Sn in this reaction is in the second excited state ($\frac{7}{2}^+$). In ref. [16] the neutrino absorbtion cross section for the production of ^{115}Sn from ^{115}In was calculated by the measured cross sections of the reaction $^{115}In(p, n)^{115}Sn$ at proton bombarding energies 120MeV and 200MeV. In the ^{115}In experiment individual electrons can be detected which can provide information about the spectra of neutrinos.

^{127}I : Haxton [18] proposed the use of ^{127}I as the active element in a solar-neutrino detector, because the reaction $^{127}I(\nu_e, e^-)^{127}Xe$ is similar to $^{37}Cl(\nu_e, e^-)^{37}Ar$ employed at Homestake experiment [1]. An additional advantage of ^{127}I is that its natural abundance is about 4 times higher than that of ^{37}Cl . In ref. [18] the sensitivity of such a detector to neutrinos coming from galactic supernova is also discussed. In ref. [20] the reduced transition probability per unit energy (strength function) and the cross section of the reaction $^{127}I(\nu_e, e^-)^{127}Xe$ are calculated in the framework of the theory of finite Fermi systems. In ref. [19] the TDA approximation is used to calculate the expected event rate for ^{127}I solar neutrino detector. One excited state in ^{127}Xe is accessible in 7Be neutrinos. For 8B neutrinos the estimates of the cross sections are based on extrapolation from data in much lighter nuclei, e.g. Haxton [18] estimated the cross section of 8B neutrinos on ^{127}I to be 6-7 times bigger than that of ^{37}Cl by extrapolating the (p,n) experimental data on ^{98}Mo and ^{71}Ga . Measurements of ^{127}I can be used to calibrate both the 8B and 7Be cross sections since ^{127}I is sensitive to both of them. ^{127}I is also a promising candidate to cover the region between ^{71}Ga and the water detector Cerenkov-chamber.

^{205}Tl : Though the neutrino capture cross section for ^{205}Tl is uncertain, there have been some interesting proposals for geochemical experiments [5,17] suggesting the measure of the concentration of the ^{205}Pb isotope produced in natural ores by solar neutrinos.

In table 1 the ingredients for the neutrino reactions $(A, Z)(\nu_l, l^-)(A, Z + 1)$ and antineutrino reactions $(A, Z)(\bar{\nu}_l, l^+)(A, Z - 1)$ studied in the present work are shown. A common advantage of these targets is that they lie in the β decay valley which avoids mixing of the β particles with those of the reactions of eq. (1) in the electron neutrino case. In columns 2 and 3 of table 1, we show the experimental nuclear distribution parameters for a two-parameter Fermi density used in eq. (6). These parameters have been obtained either directly from experimental data [41] or by interpolation using the experimental data [41] and ref. [35]. In columns 5 and 7 of table 1, we show the Q values for neutrino and antineutrino reactions calculated by using the experimental data of ref. [42].

IV. RESULTS AND DISCUSSION

In the present work we have calculated inclusive neutrino-nucleus cross sections by using Gauss integration in eq. (6). The total cross sections as a function of neutrino (antineutrino) energies obtained this way for the nuclear targets ^{37}Cl , ^{40}Ar , ^{71}Ga , ^{81}Br , ^{98}Mo , ^{115}In , ^{127}I and ^{205}Tl are presented in figs. 1-4. As we have mentioned previously, these isotopes are low-energy β emitters and either they have been used as neutrino-detection targets in experiments already being in operation or they have been proposed for feature usage.

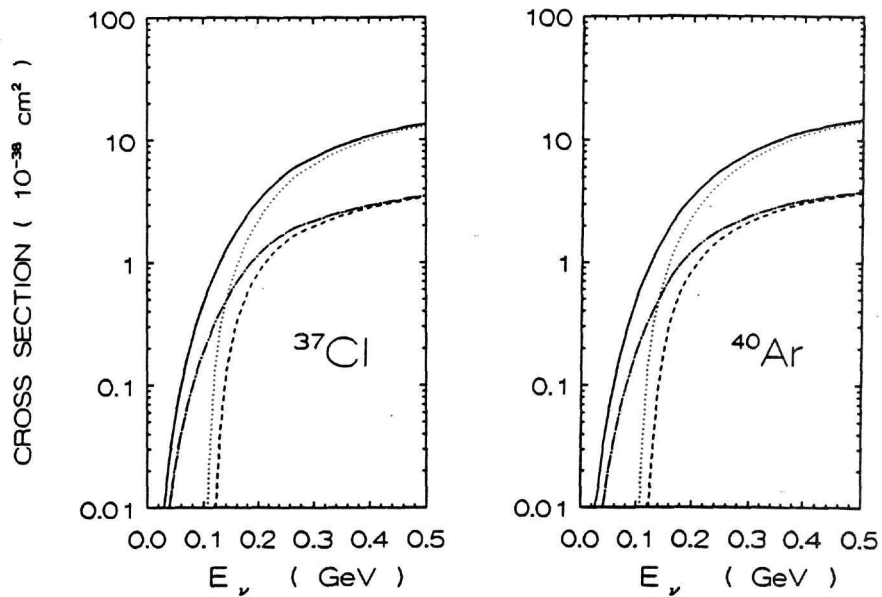


Fig. 1: Total cross sections for neutrino-nucleus reactions for ^{37}Cl target (left) and ^{40}Ar target (right). Graphs are: $^{37}Cl(\nu_e, e^-)^{37}Ar$ (solid line), $^{37}Cl(\nu_\mu, \mu^-)^{37}Ar$ (dotted line), $^{37}Cl(\bar{\nu}_e, e^+)^{37}S$ (dashed line) and $^{37}Cl(\bar{\nu}_\mu, \mu^+)^{37}S$ (dashed-dotted line).

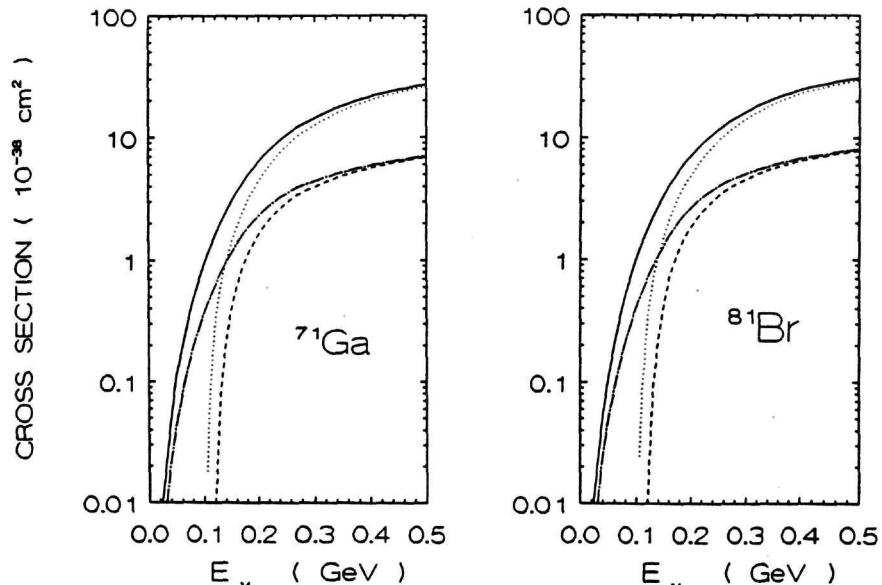


Fig. 2: Total cross sections for ^{71}Ga target (left) and for ^{81}Br (right). See fig. 1.

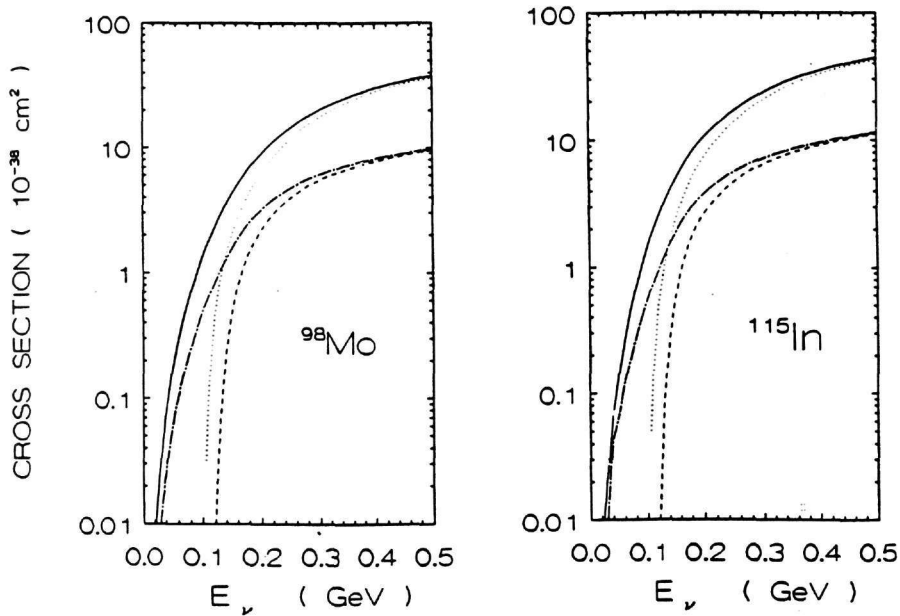


Fig. 3: Total cross sections for ^{98}Mo target (left) and for ^{115}In (right). See fig. 1.

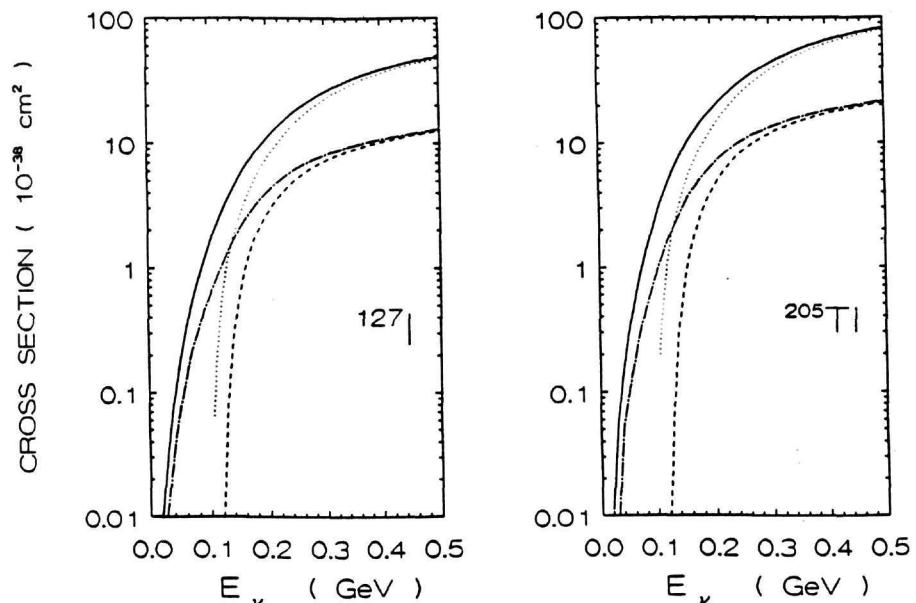


Fig. 4: Total cross sections for ^{127}I target (left) and for ^{205}Tl (right). See fig. 1.

In each of the figs. 1-4 we show the neutrino and antineutrino cross section for both the electronic- and muonic- neutrino reactions with a nuclear isotope. These results show that the neutrino and antineutrino cross section for the inclusive processes are quite sensitive to the nuclear effects in the region of intermediate energy $20\text{MeV} \leq E_\nu \leq 300\text{MeV}$ but they slowly increase in the region of $300\text{MeV} \leq E_\nu \leq 500\text{MeV}$.

We see that in the same isotope there are differences between the neutrino and antineutrino reactions as expected. For each target the electron neutrino cross sections in the region $300 \leq E_\nu \leq 500\text{MeV}$ are about equal to the corresponding muon-neutrino cross sections and the electron antineutrino cross sections are about equal to those of the muon antineutrino.

Our systematic calculations of neutrino nucleus cross sections throughout the periodic table with the accurate method of ref. [4] enables us to study the dependence of the neutrino-nucleus cross section on the nuclear charge Z and mass A . Results for the neutrino processes $(A, Z)(\nu_l, l^-)(A, Z+1)$ for some representative neutrino energies are presented and discussed in ref. [43].

Table 2. Proton emission, E_{thres}^p , and neutron emission, E_{thres}^n , energies for some neutrino detection nuclear isotopes.

Nucleus	Proton emission	Neutron emission
(A, Z)	E_{thres}^p	E_{thres}^n
(12, 7)	0.6	15.97
(37, 18)	8.72	8.80
(40, 19)	7.58	7.81
(71, 32)	8.29	7.43
(81, 36)	9.05	7.83
(98, 43)	6.18	7.29
(115, 50)	8.75	7.56
(127, 54)	7.70	7.24
(205, 82)	6.72	6.74

For a comparison of the average electron neutrino cross section $\bar{\sigma}$ extracted from experimental data at KARMEN, by using ^{127}I target [37] and at LAMPF, by using ^{12}C target [38], we need the evaluation of $\bar{\sigma}$ from eq. (12) by summing only over the particle stable excited states of the nuclei produced in the studied reactions. This means that the final nuclear states $|f\rangle$ one should include in the summation over the continuum must lie: (i) below the neutron threshold energy E_{thres}^n for the neutrino reaction and (ii) below the proton threshold energy E_{thres}^p for the antineutrino reactions. Such calculations are in progress and will appear elsewhere (see ref. [43]).

V. SUMMARY AND CONCLUSIONS

In the present work we have done a systematic study of the charged current neutrino- and antineutrino-nucleus inclusive cross sections for intermediate energies $20\text{MeV} \leq E_\nu \leq 500\text{MeV}$. We have chosen a set of eight nuclei which are very important from an experimental point of view in ongoing experiments and current proposals. We have used a reliable method which is based on the local density approximation in finite nuclei and uses the Lindhard function to take into account the effects of the Pauli blocking and Fermi motion into the nuclear medium. It also takes into consideration the renormalization of the currents involved in the process and the distortion of the Coulomb field due to the outgoing charged lepton.

We have also discussed the average cross section $\bar{\sigma}$ which for ν_e can be directly compared with the corresponding value given by experiments at KARMEN and LAMPF. Since, the method used has been checked previously in other similar reactions, the inclusive cross sections obtained in the present work are reliable and can be used in the study of neutrino detection at intermediate energies.

We would like to acknowledge partial support from the Spanish CICYT contract number AEN 93-1205 (E.O.) and the European Union Human Capital and mobility Program contract number CHRX-CT 93-0323 (T.S.K.).

References

- [1] R. Davis, Jr., D. S. Harmer, and K. C. Hoffman, Phys. Rev. **Lett.** **20**, 1205, (1968)
- [2] J. N. Bahcall et al., Phys. Rev. **Lett.** **40**, 1351, (1978)
- [3] J. N. Bahcall and R. K. Ulrich, Rev. Mod. Phys. **60**, 297, (1988)
- [4] S. K. Singh and E. Oset, Phys. Rev. **C 48**, 1246, (1993)
- [5] K. Kubodera and S. Nozawa, Int. J. Mod. Phys. **E**, to appear
- [6] R. Davis, Jr., Proc. Seventh Workshop on Grand Unification, (ICOBAN '86), Toyama, Japan, edited by J. Arafune (World Scientific, Singapore, 1987), p. 237.
- [7] R. Davis, A review of the Homestake solar neutrino experiment, Proc. Int. School on Nucl. Phys., Prog. Part. Nucl. Phys. **32** (1994)
- [8] T. Kirsten, The Gallex Experiment, Proc. 2nd workshop on neutrino telescopes, Venezia Feb. 13-15, 1990, ed. by Milla Baldo Ceolin, p. 61; L. Mosca, *ibid* p. 73; T. Kirsten, Proc. Int. School on Nucl. Phys., Prog. Part. Nucl. Phys. **32** (1994)
- [9] J. Rapaport et al., Phys. Rev. **Lett.** **47**, 1519, (1981)
- [10] A. I. Abazov et al., Phys. Rev. **Lett.** **67**, 3332, (1991)

- [11] P. Anselman *et al.*, Phys. Lett. **B 285**, 376, (1992)
- [12] R. S. Raghavan *et al.*, Phys. Rev. Lett. **76**, 259, (1976)
- [13] D. Kofcheck *et al.*, Phys. Rev. Lett. **55**, 1051, (1985)
- [14] G. S. Hurst *et al.*, Phys. Rev. Lett. **53**, 1116, (1984)
- [15] D. Kofcheck *et al.*, Phys. Lett. **B 189**, 299, (1987)
- [16] J. Rapaport *et al.*, Phys. Rev. Lett. **54**, 2325, (1985)
- [17] G. A. Cowan and W. C. Haxton, Science, **216**, 51, (1982)
- [18] W. Haxton, Phys. Rev. Lett. **60**, 768, (1988)
- [19] J. Engel, S. Pittel and P. Vogel, Phys. Rev. Lett. **67**, 426, (1991); See also preprint (1994) Phys. Rev C, submitted
- [20] Yu. S. Lutostansky and N. B. Skul'gind, Phys. Rev. Lett. **67**, 430, (1991)
- [21] W. C. Haxton, Phys. Rev. **D 36**, 2283, (1987)
- [22] J. N. Bahcall, Phys. Rev. Lett. **61**, 2650, (1988)
- [23] K. S. Hirata *et al.*, Phys. Rev. Lett. **58**, 1490, (1987); Phys. Rev. Lett. **61**, 2653, (1988); Phys. Rev. Lett. **63**, 16, (1989)
- [24] R. M. Bionta *et al.*, Phys. Rev. Lett. **58**, 1494, (1987)
- [25] T. W. Donnelly and J. D. Walecka, Phys. Lett. **B 41**, 275, (1972); T. W. Donnelly, Phys. Lett. **B 43**, 93, (1973)
- [26] J. B. Langworthy, B. A. Lamers and H. Uberall, Nucl. Phys. **A 280**, 351, (1977)
- [27] E. V. Bugaev, G. S. Bisnovatyi-Kogan, M. A. Rudzsky and Z. F. Seidov, Nucl. Phys. **A 324**, 350, (1979)
- [28] B. Gouland and H. Primakoff, Phys. Rev. **135**, B1139, (1964)
- [29] J. S. Bell and C. H. Llewellyn Smith, Nucl. Phys. **B 28**, 317, (1971)
- [30] T. K. Gaisser and J. S. O'Connell, Phys. Rev. **D 34**, 822, (1986)
- [31] T. Kuramoto, M. Fukugita, Y. Kohyama and K. Kubodera, Nucl. Phys. **A 512**, 711, (1990)
- [32] S. K. Singh and E. Oset, Nucl. Phys. **A 542**, 587, (1992)
- [33] H. C. Chiang, E. Oset and P. Fernandez de Cordoba, Nucl. Phys. **A 510**, 591, (1990)
- [34] H. C. Chiang, E. Oset, R. C. Carrasco, J. Nieves and J. Navarro, Nucl. Phys. **A 510**, 573, (1990)

- [35] E. Oset, P. Fernandez de Cordoba, L.L. Salcedo and R. Brockmann, Phys. Reports **188**, 79, (1990)
- [36] B. Bodmann *et al.*, Phys. Lett. **B 280**, 198, (1992)
- [37] G. Drexlin, Private Communication (1993)
- [38] D.A. Krakauer *et al.*, Phys. Rev. **C 45**, 2450, (1992); B.T. Cleveland, T. Daily, J. Distel, K. Lande, C.K. Lee *et al*, Proc. 23rd INter. Cosmic Ray Conference (University of Calgary, Alberta, Canada, 1993) Vol.3, p.865.
- [39] E. Oset and M. Rho, Phys. Rev. Lett. **42**, 47, (1979)
- [40] B. A. Brown, Phys. Rev. Lett. **69**, 1034, (1992)
- [41] H. de Vries, C. W. de Jager and C. de Vries, Atomic Data and Nuclear Data Tables, **36**, 495, (1987)
- [42] C. M. Lederer and V. C. Shirley, Tables of Isotopes (Wiley, New York, 1978)
- [43] T.S. Kosmas and E. Oset. in preparation.